

# A Comprehensive Approach for Evaluation of Stereo Correspondence Solutions in Augmented Reality

Bahar Pourazar and Oscar Meruvia-Pastor

*Computer Science Department, Memorial University of Newfoundland, St. John's, Canada*

**Keywords:** Augmented Reality, Human Visual System, Binocular Stereo, Stereoacuity, Disparity, Stereo Correspondence.

**Abstract:** This paper suggests a comprehensive approach for the evaluation of stereo correspondence techniques based on the specific requirements of outdoor augmented reality systems. To this end, we present an evaluation model that integrates existing metrics of stereo correspondence algorithms with additional metrics that consider human factors that are relevant in the context of outdoor augmented reality systems. Our model provides modified metrics of stereoacuity, average outliers, disparity error, and processing time. These metrics have been modified to provide more relevant information with respect to the target application. We evaluate our model using two stereo correspondence methods: the OpenCV implementation of the semi-global block matching, also known as SGBM, which is a modified version of the semi-global matching by Hirschmuller; and our implementation of the solution by Mei et al., known as ADCensus. To test these methods, we use a sample of fifty-two image pairs selected from the Kitti stereo dataset, which depicts many situations typical of outdoor scenery. Experimental results show that our proposed model can provide a more detailed evaluation of both algorithms. Further, we discuss areas of improvement and suggest directions for future research.

## 1 INTRODUCTION

Many Augmented Reality (AR) systems require some form of optical markers placed within a scene in order to integrate computer-generated objects with scenery directly generated from the real world; these markers help the system identify the location of an item within the scene to be used as a place-holder for the synthetic objects. Placing such markers in objects that are part of a scene may work for many indoor environments, but is a less practical option in outdoor AR settings where users can move freely in their surroundings. In the absence of such markers, an AR system requires a depth map of the surrounding environment. In order to obtain the 3D location of different objects in the scene, several technologies can be used. Among these technologies, one of the most practical techniques is the use of stereo cameras to take images of the scene from slightly different viewpoints. These images can then be processed by the stereo correspondence algorithms, which attempt to find the corresponding pixels in the stereo images, to generate the depth map of the surrounding environment. This map is then used to integrate virtual objects in the scene such that synthetic objects are rendered in a way that considers the occlusion properties and the depth of the real objects in the scene. Due to the potential applications of stereo

correspondence, which is one of the most extensively studied subjects in computer vision (Scharstein and Szeliski, 2002), using an evaluation scheme that is designed according to the specific requirements of the target application is essential. The evaluation scheme proposed in this paper is designed for outdoor AR applications which make use of stereo vision techniques to obtain a depth map of the surrounding environment.

Over the past few years, a few evaluation schemes have been proposed by researchers in the field to provide a testbed for assessment of the solutions based on specific criteria. The Middlebury Stereo (Daniel Scharstein, 2012) and the Kitti Stereo benchmarks (Andreas Geiger, 2012) are two of the most popular and widely used evaluation systems through which a stereo correspondence algorithm can be evaluated and compared to others. However, both of these models take a general approach towards evaluating the methods; that is, they have not been designed with an eye to any particular target application. In fact, these models focus on the particular application of a stereo correspondence algorithm as a solution per se to find the *best matches* of the corresponding pixels in stereo pairs, regardless of the target application. However, the information provided by these evaluation benchmarks is not sufficient to select

a given algorithm suitable for AR, because we need information on the specific *accuracy* and *efficiency* of these algorithms, for example to assess their suitability regarding their processing time. The fact that some of this information is missing from such standard evaluations of stereo correspondence methods has compelled us to take steps towards a comprehensive evaluation design based on specific requirements of outdoor stereo AR applications, which results in better definition and adjustment of the criteria for efficiency and accuracy metrics used for the evaluation.

## 2 BACKGROUND AND TERMINOLOGY

Over the past decades, many mobile AR systems have been built, from the Touring Machine in 1997 (Feiner et al., 1997) to Google Glass which was announced in 2013 (Google Inc., 2013); however, most of these prototypes have remained experimental due to certain difficulties and constraints of using them in practical applications (Drascic and Milgram, 1996; Livingston, 2005). Two of the most important constraints are the human factors in AR and the high demand of computational resources needed to provide a real-time interaction between the user and the system; therefore, in order to build a practical AR system, these factors need to be carefully considered while designing different components of the system.

### 2.1 Binocular Vision and the Human Visual System

Studies in binocular vision show that human perception of depth can vary depending on the environment and under different circumstances. Many studies have focused on the evaluation of human perception of depth within different frameworks and in different applications, such as virtual reality and AR, which have recently attracted more attention (Wann et al., 1995; Drascic and Milgram, 1996; Livingston, 2005; Jerome and Witmer, 2005; Swan et al., 2007; Kruijff et al., 2010). These studies show that the viewer perception of depth is inversely proportional to his/her distance from the object (Kruijff et al., 2010; Swan et al., 2007; Jerome and Witmer, 2005; Livingston, 2005); for instance, in (Swan et al., 2007), some experiments are designed to study and evaluate the human perception of distance, in terms of the absolute depth of the objects from the observer, for an outdoor AR application in urban settings. However, in this research we are more interested in the human percep-

tion of relative depth in stereo vision: the ability to perceive and distinguish the depth of different objects relative to each other. In binocular vision, the minimum depth difference between two points that can be detected in the visual system is known as *Stereoscopic Acuity* or *Stereoacuity* (Pfautz, 2000). This metric is normally presented in angular units, commonly arcseconds. According to the geometry of binocular vision illustrated in Figure 1, stereoacuity can be obtained from the following equation:

$$\theta = \frac{a\Delta Z}{Z^2} \quad (1)$$

This equation estimates the angular disparity in radians, where  $a$  is the distance between the center of the pupils of the two eyes, which is known as interpupillary distance.

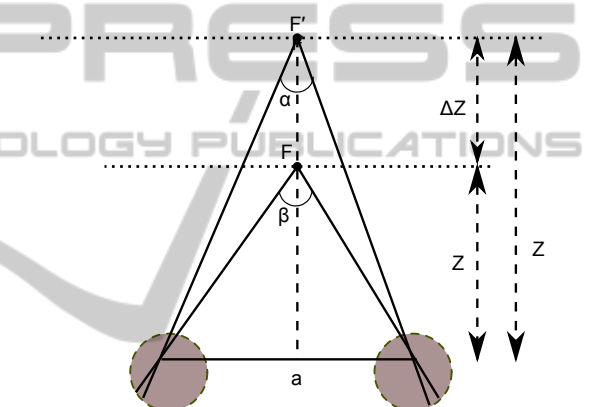


Figure 1: Binocular disparity.

According to standard stereo tests (Reading, 1983), the finest detectable disparity in the human visual system (HVS) is approximately 10-15 arcseconds. However, a more recent study on 60 subjects (Garnham and Sloper, 2006) at different age groups, from 17 to 83 using standard stereotests, shows that the average stereoacuity for different age groups is as follows:

Table 1: Average stereoacuity for subjects ages 17 to 83.

Age Range	Avg. Stereoacuity(arcsecs)
17-29	32
30-49	33.75
50-69	38.75
70-83	112.5

As can be seen, the stereoacuity for the HVS increases with age, that is the amount of error in the depth results is less perceptible in the visual system of the elders than the younger people. Using these values in Equation 1 along with the average interpupillary

distance in the human visual system, that is approximately 64mm (Howard and Rogers, 1995), we can estimate the threshold for minimum detectable depth between two objects based on their distance from the observer.

## 2.2 Real-time Interaction

Providing real-time interaction in an AR system for the user requires the processing time and update rate of the whole system to keep up ideally with the standard video frame rate, between 24fps and 30fps, or higher. However, studies show that in practice to build a reasonable interactive augmented world the processing rate should not be less than half of the video frame rate (Hertzmann and Perlin, 2000). Two ways to speed up a system are using a more advanced technology and hardware, and implementing more sophisticated and efficient software design. However, having access to advanced technology and hardware is not always feasible and even the most advanced technologies have some limitation in their memory space and computational capability which may not meet the requirement for some real-time applications. Therefore, in many cases, employing the second approach is more practical.

## 3 COMPREHENSIVE EVALUATION SCHEME

In our design, unlike the Middlebury or Kitti benchmarks, we label a pixel in the disparity results as an *outlier* if the angular measurement, that is the stereoacuity, corresponding to the depth error between the ground truth and the estimated depth value by the algorithm is more than the average perceptible stereoacuity of the HVS as determined by standard stereo tests (Reading, 1983; Garnham and Sloper, 2006). Moreover, we use the average stereoacuity for different age groups (Garnham and Sloper, 2006) in our design to evaluate the performance of the algorithm for users at different ages; this makes the evaluation results more reliable and applicable to applications of AR. In order to evaluate the efficiency of an algorithm and investigate whether it meets the requirements for being part of a real-time AR application, we integrate a module in the evaluation process that reports on the average execution time of the algorithm for the input data. The average outliers based on the specified stereoacuity thresholds and the average disparity error are also estimated during the evaluation process.

In addition, our model employs a particular approach which can be of specific value to AR applications. In this approach, we suggest that it is important to focus the evaluation process on particular regions of the disparity map rather than the whole image. The main reason is that salient edges caused by depth discontinuities, which also represent object boundaries and occlusion, are important depth cues for the human visual system to better perceive the location of different objects in the 3D environment (Szeliski, 2011). Therefore, more accurate depth results in these regions permits a higher quality combination of the depth map of the real world with the virtual depth of the synthetic objects that are part of the AR scene. To this end, we build a mask using the ground truth disparity map which is, in fact, a mask of the edges in the image caused by depth discontinuities and their surrounding area.

### 3.1 Architecture

The block diagram of our evaluation system can be seen in Figure 2, which illustrates the sequence of the operations during the whole process. As can be seen in this figure, first the input data consisting of the stereo images, the ground truth disparity, and the calibration data are passed to the system. Afterwards, the specified masks are created using a *Canny* edge detector and a *Dilation* operation with the appropriate parameters selected separately for each image. After the corresponding disparity maps have been generated by the stereo algorithm and stored on the disk, they are passed to the evaluation module with the specified arguments. Finally, the evaluation metrics are estimated and output as data files and plots to facilitate the evaluation of the stereo algorithm in the application of interest.

### 3.2 Evaluation Metrics

The main evaluation component consists of different modules which estimate specific evaluation metrics. These metrics are: 1) the average stereoacuity, 2) the average outliers, 3) the average disparity error, and 4) the average execution time. Analysis of these metrics in the framework of an outdoor AR application will then allow for a practical evaluation of the stereo algorithm performance.

#### 3.2.1 Average Stereoacuity

We can break the estimation of the average stereoacuity down to 3 steps: 1) estimate the stereoacuity based on the generated disparity for each image pair and

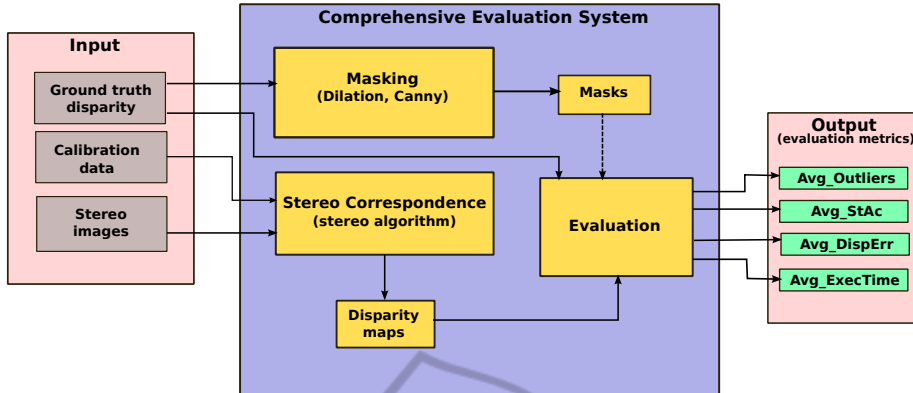


Figure 2: Architecture of the evaluation system.

the ground truth; 2) average the stereoacuity results over certain depth ranges in each image; 3) average the results from the previous step over all the images. Corresponding plots are generated after the third step based on the final results.

According to the specific age ranges, different values are reported for the average stereoacuity at the end of the evaluation. In order to estimate this metric, the depth values corresponding to both ground truth and the generated disparity by the algorithm are first calculated. Subsequently, the difference between these values is used in Equation 1 to calculate the corresponding stereoacuity, Equations 2 and 3. This process is done for all the pixels in the image; or if a mask has been provided, it will be applied only to the pixels in the masked areas. Finally the results are output and stored in a separate data file for each image.

$$Depth_{err} = |depth_{gt} - depth_{gen}| \quad (2)$$

$$StAc = \frac{a * Depth_{err}}{depth_{gt}^2} \quad (3)$$

Here,  $depth_{gt}$ ,  $depth_{gen}$ ,  $StAc$  and  $a$  denote the ground truth depth, the generated depth by the algorithm, the corresponding stereoacuity, and the average interpupillary distance, respectively.

After conducting the first step on all the disparity maps corresponding to input image pairs, the second step starts by building a histogram of the stereoacuity values over specific depth ranges, Equations 5 and 6. In our design, the width of each bin determines the aforementioned depth range and is kept constant for all the bins. Moreover, the number of bins along with their corresponding width determine the total distance over which the results are estimated and subsequently examined.

$$Total\_distance = Number\_of\_bins * Width \quad (4)$$

For outdoor applications of AR, these parameters are normally set to certain values so that the total distance

covers the medium to far depth fields; extending from 1.5 meters to more than 30 meters (Swan et al., 2007).

$$Sum_{dRange} = \sum_{dRange} StAc \quad (5)$$

$$Avg\_StAc_{dRange} = \frac{Sum_{dRange}}{(NumOfPixels_{dRange})} \quad (6)$$

Here,  $Avg\_StAc_{dRange}$  and  $Sum_{dRange}$  denote the average and total stereoacuity over specified depth ranges in each image, and  $NumOfPixels_{dRange}$  denote the number of pixels within each depth range.

The results of the previous step, all stored in a data file, are then passed to the last step. At this point, a histogram is built over the data from all the disparity images, which results in the average stereoacuity values within each specified depth range over all the images, Equation 7. It should be noted that the number of bins and their corresponding width in this step are similar to the histogram constructed in the previous step.

$$Avg\_StAc = \frac{\sum_{imgs}(Sum_{dRange})}{\sum_{imgs}(NumOfPixels_{dRange})} \quad (7)$$

### 3.2.2 Average Outliers

For this measurement, the relative depth error is first calculated by finding the corresponding depth values for the ground truth disparity and the disparity generated by the algorithm and then converted to effective stereoacuity, as shown in Equations 2 and 3. This value is then compared to the relative detectable depth threshold for the HVS that is estimated using Equation 1. If the relative depth error is equal to or more than the detectable threshold in the HVS, Equation 8, then the corresponding pixel is labelled as an outlier.

$$StAc \geq StAc_{threshold} \quad (8)$$

Since we are using four different thresholds of stereoacuity corresponding to different age groups



Figure 3: Sample outdoor scene from the Kitti stereo dataset (Andreas Geiger, 2012). Top: left image. Bottom: right image.

in our evaluation, the estimated error is compared against each of these thresholds, and therefore, four different values are eventually calculated. The average outliers is then computed as a fraction of the total number of pixels in the inspected regions, Equation 9.

$$\text{Avg\_Outliers} = \frac{\text{Outliers}_{\text{total}}}{\text{NumOfPixs}} \quad (9)$$

This process is repeated for all the pixels in the image or merely the pixels in the masked regions depending on the availability of a mask.

### 3.2.3 Average Disparity Error

This metric is the mean error between the ground truth disparity and the one found by the algorithm, which is estimated for all the pixels in the image or merely the masked pixels depending on the availability of a mask. It can be presented with the following estimations:

$$\text{Disp}_{\text{err}} = | \text{disp}_{\text{gt}} - \text{disp}_{\text{gen}} | \quad (10)$$

$$\text{DispErr}_{\text{total}} = \sum_{\text{pixs}} \text{Disp}_{\text{err}} \quad (11)$$

After the computation of the total disparity error for the pixels, the average disparity error is estimated as follows:

$$\text{Avg\_DispErr} = \frac{\text{DispErr}_{\text{total}}}{\text{NumOfPixs}} \quad (12)$$

The *NumOfPixs* is, in fact, the total number of pixels in the whole image or the masked regions, depending on the case for which the error is being estimated.

### 3.2.4 Average Execution Time

We use the C++ function *clock()* to estimate the average execution time of the algorithms for generating disparity results corresponding to the input stereo images, fifty-two image pairs in our evaluation. We then compare this value to the acceptable criteria for having a real-time interactive AR system from the user's perspective, that is, a processing time less than 0.06–0.08 seconds per frame corresponding to a frame rate of 12.5 to 16.5 fps, as proposed by (Hertzmann and Perlin, 2000).

Analyzing each of these metrics in the light of the relevant factors in an outdoor AR application results in a practical evaluation of the stereo correspondence methods.

## 4 VALIDATION

In order to verify the effectiveness of our proposed model for the evaluation of stereo correspondence methods in outdoor AR applications, we have evaluated two sample stereo algorithms: the OpenCV implementation of the semi-global block matching, also

known as SGBM, which is a modified version of the semi-global matching by Hirschmuller (Hirschmuller, 2008); and our implementation of “on building an accurate stereo matching system on graphics hardware” (Mei et al., 2011), also known as ADCensus. It should be noted that the CPU implementation of both methods have been used.

Experiments were carried out on a Linux platform with Intel Core(TM) i7 3.20GHz CPU. Fifty-two image pairs were chosen from the Kitti Stereo Dataset corresponding to real outdoor scenes. Figure 3 shows a sample stereo pair from the Kitti dataset. The OpenCV Canny edge detector and Dilation operation were used for building the specified masks and the expansion of the masked areas, respectively. Parameters corresponding to stereo algorithms, the aperture size in Canny, and the degree of Dilation were kept constant over all the images and experiments. These values are presented in Tables 2, 3, and 4. The parameters for Dilation and Canny were chosen empirically by running the algorithms over our image set with the intention of selecting the values which best define the depth edges and expand them enough to include regions with different depths surrounding the edges.

Table 2: SGBM Parameters.

SADWindowSize	9
disp12MaxDiff	2
uniquenessRatio	10
P2	3*9
speckleWindowSize	100
speckleRange	2

Table 3: ADCensus Parameters.

$\lambda_{AD}$	10	$\lambda_{Census}$	30	$L_1$	34	$L_2$	17
$\tau_1$	20	$\tau_2$	6	$\pi_1$	1.0	$\pi_2$	3.0
$\tau_{SO}$	15	$\tau_S$	20	$\tau_H$	0.4		

Table 4: Masking Parameters.

Dilation_iterations	10
Canny_apertureSize	3

The minimum and maximum disparity values are also kept constant for each image pair in both algorithms; however, the maximum disparity differ for each image pair as the scenes are different and objects are located at different depth fields. The minimum disparity is set to 0 for both algorithms. The maximum disparity for each image pair is selected based on the maximum value in their corresponding ground truth disparity. The standard stereoacuities used for the evaluation are based on the results mentioned in Table 1.

## 4.1 Experimental Results

The evaluation metrics, mentioned in Section 3.2, were estimated for SGBM and ADCensus in our evaluation system. The main results are described below.

### 4.1.1 Average Stereoacuity

Figures 4 and 5 show the average relative depth error converted to effective stereoacuity over distance for the masked and the whole images with both SGBM and ADCensus.

In these plots, a cross point below a stereoacuity threshold (straight lines) implies that the average error in the disparity values estimated by the stereo algorithm is imperceptible to the human visual system. However, a value higher than the threshold indicates that the error cannot be ignored and should be resolved to achieve a better alignment between the virtual and the real world in the AR application of interest. Moreover, as can be seen most of the errors fall below the standard stereoacuity value corresponding to older ages; indicating that these are not perceptible to the visual system of people at these particular ages. The zero values in the plots imply that either there is no object within the corresponding range or the disparity value estimated by the algorithm is equal to the ground truth disparity; however, since the average of the results has been taken over all the images, it is more likely that the zero values indicate no object within the particular range.

As can be seen in the results, SGBM performs better in finding more accurate corresponding matches compared to ADCensus, as most of the error points fall below the standard stereoacuity lines. Moreover, the plots show that in both methods the significant amount of error corresponds to the near field objects, within the first 5 meters. This range of the depth field can be considerably important in some applications, such as the ones involving certain manipulative tasks; for these types of applications, other technologies, such as depth sensing cameras, are better choice.

Comparing the results between the masked and the whole image show that the average error over the masked regions; that is, near the depth edges, is very similar to the results over the whole image. This may imply that there is no additional benefit in the inspection of these regions. However, this might be merely an indication of the performance of the selected algorithms and can be better analyzed by evaluating more algorithms within our model.

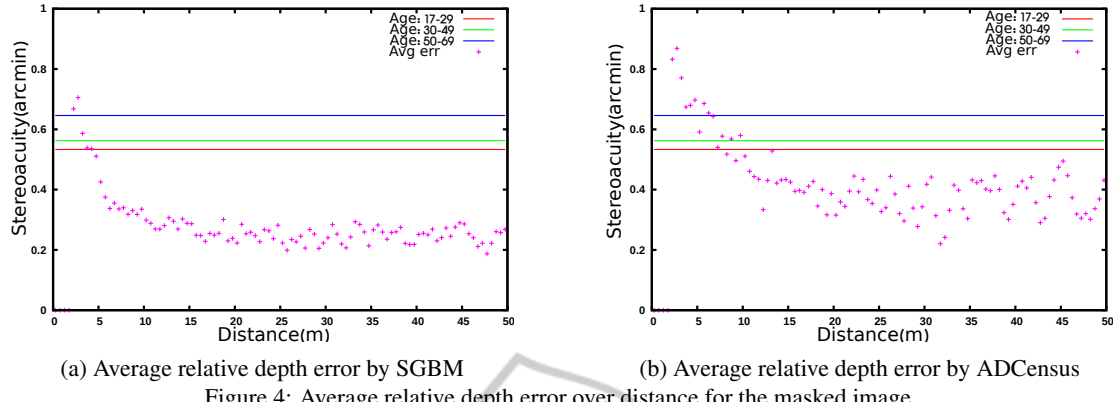


Figure 4: Average relative depth error over distance for the masked image.

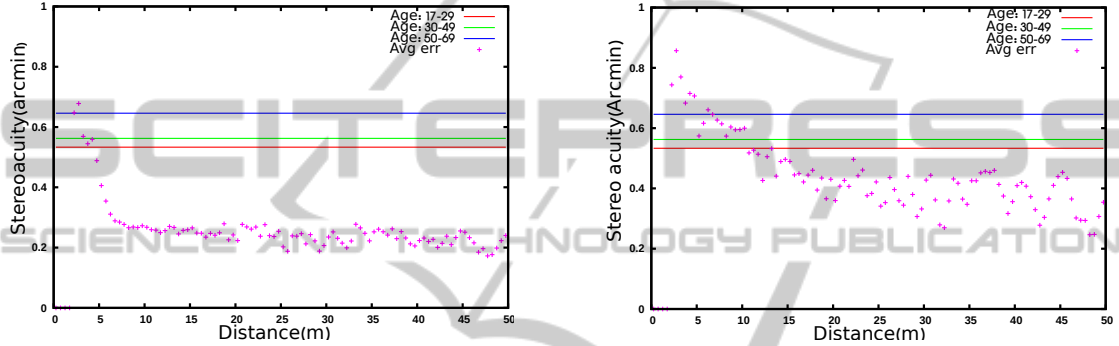


Figure 5: Average relative depth error over distance for the whole image.

#### 4.1.2 Average Outliers

The average outliers for the masked and the whole image are presented in Table 5. Results show that in both cases, the masked regions and the whole image, SGBM has less average outliers than ADCensus, indicating that SGBM generates a more accurate disparity map as perceived by the human visual system.

Another observation is that in SGBM, the average outliers over the masked regions is larger than the average outliers over the whole image, whereas in ADCensus the opposite behavior is observed. This implies that SGBM generates less accurate results near the depth discontinuities and occluded regions compared to the other areas in the image. On the other hand, ADCensus generates more accurate disparity values near the depth edges compared to the other regions in the image and tends to preserve the occluded regions. This only indicates that, despite the better performance of SGBM over ADCensus according to the experimental results, in cases where only one of these solutions is available, it is reasonable to consider this behavior to employ the method in the right application based on the accuracy requirement of the target system in different regions. In other words, it is important to first investigate

which regions of the image are more important in the context of the target application. For instance, ADCensus performs better in an application where the areas near depth discontinuities and occlusion are more important than the rest of the image, such as image compositing for layering visual elements on the scene, compared to application scenarios where obtaining an accurate, dense disparity map for all the regions in an image is essential, such as constructing a 3D model of the scene or preparing a model for 3D printing. Figure 6 shows a comparison of all the results.

#### 4.1.3 Average Disparity Error

The average disparity error for both the whole and the masked image are presented in Table 6. As can be seen, ADCensus results in less average disparity error than SGBM. This difference is likely caused by the various refinement steps implemented in the ADCensus algorithm which do not exist in SGBM. As a result, despite the larger outliers in ADCensus than SGBM as presented in Section 4.1.2, ADCensus attempts to decrease the difference between the resulting disparity value and the ground truth dispar-

Table 5: Average outliers.

Algorithm	Age	Average Outliers(Masked)	Average Outliers(Full)
SGBM	17-29	0.12	0.11
	30-49	0.11	0.10
	50-69	0.09	0.08
	70-83	0.0012	0.005
ADCensus	17-29	0.23	0.27
	30-49	0.22	0.26
	50-69	0.18	0.22
	70-83	0.002	0.002

Table 6: Average disparity error.

Algorithm	Region	Avg_DispNet
SGBM	Full	6.58
	Masked	7.81
ADCensus	Full	4.49
	Masked	4.74

ity through multiple refinement steps, thus generating smoother disparity patches within different regions of the image. Figure 7 presents a comparison between all the results.

#### 4.1.4 Average Execution Time

In another experiment, we estimated the average execution time for both algorithms using a set of fifty-two stereo image pairs from the Kitti data set (Andreas Geiger, 2012). Results of the average execution time over all the images are shown in Table 7. Considering the requirements of a real-time AR system (Hertzmann and Perlin, 2000), the processing time of each frame should not be more than 0.06-0.08 seconds. Although the current implementation of SGBM could be used when the real world scene remains stable for approximately one second, it can be safely concluded that none of these implementation meets the requirements of a real-time interactive AR system.

Table 7: Average execution time.

Algorithm	Avg_ExecTime(secs)
SGBM	0.54
ADCensus	272.82

## 4.2 Overview

Table 8 shows an overview of the difference between our proposed evaluation approach and the other evaluation models, Middlebury and Kitti, in terms of the estimated evaluation metrics.

It should be noted that although the average error and the average outliers exist in the other evaluation schemes as well, the major difference which makes

our evaluation more appropriate than the other schemes for practical applications of AR, is the approach employed during the design of the metrics and the analysis of the results in the evaluation process. In fact, integrating the important factors related to the human visual system and its perception of depth in the design of the metrics and the insights they provide make the evaluation model more relevant and applicable to outdoor AR systems.

Table 8: Comparison of different evaluation schemes.

Metrics	Evaluation Models		
	Middlebury	Kitti	Comprehensive Evaluation
Avg_StAc	✗	✗	✓
Avg_Outliers	✓	✓	✓
Avg_DispNet	✓	✓	✓
Avg_ExecTime	✗	✗	✓

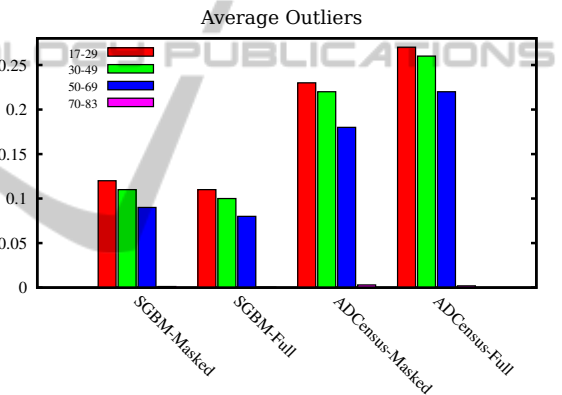


Figure 6: Average outliers for both SGBM and ADCensus.

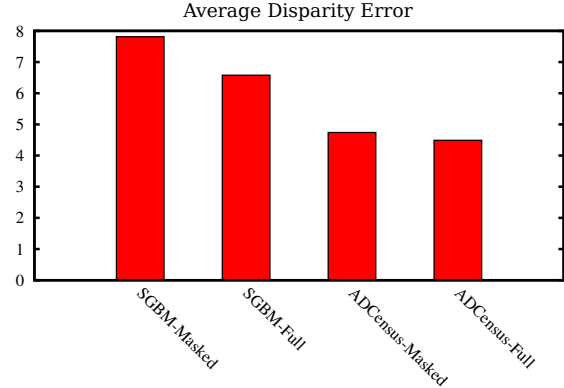


Figure 7: Average disparity error for both SGBM and ADCensus.

## 5 CONCLUSION

In this paper, we present a new approach for evaluating stereo algorithms in which we suggest that evaluation metrics should be designed or chosen based on the specific requirements of the target application. We then applied this concept to the particular application of augmented reality systems in outdoor environments. We chose outdoor environments because these environments pose additional challenges to stereo vision algorithms and AR systems since they must cope with external factors that cannot be easily controlled, such as the effects of shadows, illumination and weather. As a result, a practical analysis on the performance of the stereo algorithms, in terms of *accuracy* and *processing time* as perceived by the HVS, was presented. The results over the masked regions did not show any significant benefit to the evaluation of the areas near the depth discontinuities and occluded regions; however, as mentioned previously, this might be merely an indication of the performance of the algorithms we selected for evaluation and can only be better analyzed by evaluating more algorithms within our model. In either case, we hypothesize that, due to the importance of occlusion and areas near depth discontinuities to the HVS for the perception of depth in AR applications, it might be reasonable to focus more on the regions that contain depth edges and their surroundings when designing or employing a stereo matching technique for an AR application. Validation of this hypothesis is a topic we would like to further investigate in the future research. Moreover, we would like to assess the benefits of our model for other AR applications, such as underwater environments, and explore other factors which may also affect the evaluation process, such as the resolution of the display device, and the effect of contrast and brightness.

## ACKNOWLEDGEMENTS

The authors would like to thank the Research and Development Corporation (RDC) of Newfoundland and Labrador, which provided the funding for the project, and also Dr. Paul Gilliard, for his advice and support for this project.

## REFERENCES

Andreas Geiger (2012). KITTI Vision.<http://www.cvlibs.net/datasets/kitti/>.

- Daniel Scharstein (2012). MiddleBury Evaluation.<http://vision.middlebury.edu/stereo/eval/>.
- Drascic, D. and Milgram, P. (1996). Perceptual issues in augmented reality. In *Electronic Imaging: Science & Technology*, pages 123–134. International Society for Optics and Photonics.
- Feiner, S., MacIntyre, B., Höllerer, T., and Webster, A. (1997). A touring machine: Prototyping 3d mobile augmented reality systems for exploring the urban environment. *Personal Technologies*, 1(4):208–217.
- Garnham, L. and Sloper, J. (2006). Effect of age on adult stereoauity as measured by different types of stereotest. *British journal of ophthalmology*, 90(1):91–95.
- Google Inc. (2013). Google AR Glasses. <http://www.google.com/glass/start/>.
- Hertzmann, A. and Perlin, K. (2000). Painterly rendering for video and interaction. In *Proceedings of the 1st International Symposium on Non-photorealistic Animation and Rendering*, NPAR '00, pages 7–12, New York, NY, USA. ACM.
- Hirschmuller, H. (2008). Stereo processing by semiglobal matching and mutual information. *Pattern Analysis and Machine Intelligence, IEEE Transactions on*, 30(2):328–341.
- Howard, I. P. and Rogers, B. J. (1995). *Binocular vision and stereopsis*. Oxford University Press.
- Jerome, C. and Witmer, B. (2005). The perception and estimation of egocentric distance in real and augmented reality environments. In *Proceedings of the Human Factors and Ergonomics Society Annual Meeting*, volume 49, pages 2249–2252. SAGE Publications.
- Kruijff, E., Swan, J., and Feiner, S. (2010). Perceptual issues in augmented reality revisited. In *Mixed and Augmented Reality (ISMAR), 2010 9th IEEE International Symposium on*, pages 3–12. IEEE.
- Livingston, M. A. (2005). Evaluating human factors in augmented reality systems. *Computer Graphics and Applications, IEEE*, 25(6):6–9.
- Mei, X., Sun, X., Zhou, M., Jiao, S., Wang, H., and Zhang, X. (2011). On building an accurate stereo matching system on graphics hardware. In *Computer Vision Workshops (ICCV Workshops), 2011 IEEE International Conference on*, pages 467–474. IEEE.
- Pfautz, J. D. (2000). *Depth perception in computer graphics*. PhD thesis, University of Cambridge.
- Reading, R. (1983). *Binocular vision: Foundations and applications*. Butterworths.
- Scharstein, D. and Szeliski, R. (2002). A taxonomy and evaluation of dense two-frame stereo correspondence algorithms. *International journal of computer vision*, 47(1-3):7–42.
- Swan, J. E., Jones, A., Kolstad, E., Livingston, M. A., and Smallman, H. S. (2007). Egocentric depth judgments in optical, see-through augmented reality. *Visualization and Computer Graphics, IEEE Transactions on*, 13(3):429–442.
- Szeliski, R. (2011). *Computer vision: algorithms and applications*. Springer.
- Wann, J. P., Rushton, S., and Mon-Williams, M. (1995). Natural problems for stereoscopic depth perception in virtual environments. *Vision research*, 35(19):2731–2736.